Cancer Therapy: Preclinical

Clinical Cancer Research

BMN 673, a Novel and Highly Potent PARP1/2 Inhibitor for the Treatment of Human Cancers with DNA Repair Deficiency

Yuqiao Shen[1], Farah L. Rehman[2,3], Ying Feng[1], Julia Boshuizen[2,3], Ilirjana Bajrami[2,3], Richard Elliott[2,3], Bing Wang[1], Christopher J. Lord[2,3], Leonard E. Post[1], and Alan Ashworth[2,3]

Abstract

Purpose: PARP1/2 inhibitors are a class of anticancer agents that target tumor-specific defects in DNA repair. Here, we describe BMN 673, a novel, highly potent PARP1/2 inhibitor with favorable metabolic stability, oral bioavailability, and pharmacokinetic properties.

Experimental Design: Potency and selectivity of BMN 673 was determined by biochemical assays. Anticancer activity either as a single-agent or in combination with other antitumor agents was evaluated both *in vitro* and in xenograft cancer models.

Results: BMN 673 is a potent PARP1/2 inhibitor (PARP1 $IC_{50} = 0.57$ nmol/L), but it does not inhibit other enzymes that we have tested. BMN 673 exhibits selective antitumor cytotoxicity and elicits DNA repair biomarkers at much lower concentrations than earlier generation PARP1/2 inhibitors (such as olaparib, rucaparib, and veliparib). *In vitro*, BMN 673 selectively targeted tumor cells with *BRCA1*, *BRCA2*, or *PTEN* gene defects with 20- to more than 200-fold greater potency than existing PARP1/2 inhibitors. BMN 673 is readily orally bioavailable, with more than 40% absolute oral bioavailability in rats when dosed in carboxylmethyl cellulose. Oral administration of BMN 673 elicited remarkable antitumor activity *in vivo*; xenografted tumors that carry defects in DNA repair due to *BRCA* mutations or PTEN deficiency were profoundly sensitive to oral BMN 673 treatment at well-tolerated doses in mice. Synergistic or additive antitumor effects were also found when BMN 673 was combined with temozolomide, SN38, or platinum drugs.

Conclusion: BMN 673 is currently in early-phase clinical development and represents a promising PARP1/2 inhibitor with potentially advantageous features in its drug class. *Clin Cancer Res; 19(18); 5003–15. ©2013 AACR.*

Introduction

DNA is constantly exposed to a range of environmental and endogenous factors that result in DNA damage (1). The repair of the resultant DNA lesions is mediated by a variety of mechanisms, including base excision repair, mismatch repair, nucleotide excision repair, homologous recombination, nonhomologous end joining, and direct reversal (1). Cancer cells often display deficiencies in one or more of these DNA repair pathways and these DNA repair defects can render tumor cells more susceptible to pharmaceutical intervention of the remaining DNA repair pathways than normal cells (2).

PARP1 and the similar enzyme PARP2 play important roles in DNA repair (3). DNA strand breaks result in the recruitment and binding of PARP1/2 to DNA at the site of damage. DNA-bound PARP1/2 catalyzes the synthesis of poly(ADP-ribose) (PAR) onto a range of DNA-associated proteins that mediate DNA repair. PARP1 also undergoes auto-PARsylation, a molecular change that ultimately leads to its release from DNA. Small-molecule inhibitors of PARP1/2 represent a class of anticancer agents that exert their cytotoxic effect by modulating the PARsylation activity of PARP1/2 (4). Inhibition of PARP1/2 is synthetically lethal with loss-of-function of either the *BRCA1* or *BRCA2* tumor suppressor genes, an effect that enables tumor cells with *BRCA* gene defects to be selectively targeted with PARP1/2 inhibitors (5). It is believed that loss of *BRCA1/2* gene function causes a deficiency in homologous recombination–mediated double-strand DNA break repair (DSBR), making these cells highly susceptible to DNA lesions caused by PARP inhibition (4, 6, 7). In the clinic, phase I and II studies have shown that the PARP1/2 inhibitor olaparib (AstraZeneca/KuDOS) can elicit significant

Authors' Affiliations: [1]BioMarin Pharmaceutical Inc., Novato, California; [2]Cancer Research UK Gene Function Laboratory; and [3]The Breakthrough Breast Cancer Research Centre, The Institute of Cancer Research, London, United Kingdom

Note: Supplementary data for this article are available at Clinical Cancer Research Online (http://clincancerres.aacrjournals.org/).

Corresponding Authors: Yuqiao Shen, BioMarin Pharmaceutical Inc., 105 Digital Drive, Novato, CA 94949. Phone: 415-506-3317; Fax: 415-382-7889; E-mail: jshen@bmrn.com; Christopher J. Lord, Chris.Lord@icr.ac.uk; and Alan Ashworth, Alan.Ashworth@icr.ac.uk

doi: 10.1158/1078-0432.CCR-13-1391

Translational Relevance

PARP1/2 inhibitors are a class of anticancer drugs that target tumor-specific defects in DNA repair. Here, we describe a novel PARP1/2 inhibitor, BMN 673, which shares features such as tumor selectivity with existing inhibitors but has strikingly increased antitumor potency and markedly improved pharmacokinetic attributes. The anticancer activity and selectivity of existing PARP1/2 inhibitors has been proven in early proof-of-concept clinical trials where patient benefit has been seen with limited toxicity. However, research to define patient selection, scheduling, and whether these agents should be used in combination with other anticancer drugs is still ongoing. BMN 673 is already being assessed in clinical trials and represents an exciting new PARP1/2 inhibitor at a time when optimal clinical use of these agents is being established.

and sustained antitumor responses as a single agent in patients with cancer with *BRCA1*- or *BRCA2*-mutant tumors, while still achieving a favorable toxicity profile (4, 8–10). Furthermore, in a phase II study in high-grade serous ovarian cancer, olaparib reduced the risk of recurrence when used as a maintenance therapy after chemotherapy (11).

PARP1/2 inhibitors have also been shown to sensitize tumor cells to cytotoxic drugs such as the alkylating agents, temozolomide and cyclophosphamide, and the topoisomerase I inhibitors, irinotecan and topotecan (12, 13). This characteristic forms the basis of potential combination therapies where PARP1/2 inhibitors could be used together with DNA-damaging anticancer agents to enhance the antitumoral response.

There are currently at least seven PARP inhibitors at various stages of clinical development (4). Here, we report the characteristics of a new, potent, and selective PARP1/2 inhibitor, BMN 673. BMN 673 exhibits many of the biochemical and cytotoxic profiles found with earlier generation PARP1/2 inhibitors such as olaparib (AZD2281, KU0059436; AstraZeneca/KuDOS), rucaparib (AG-014699, PF-01367338; Clovis/Pfizer), and veliparib (ABT-888; Abbott Laboratories). However, BMN 673 is able to achieve antitumor cell responses and elicit DNA repair biomarkers at much lower concentrations than these other PARP1/2 inhibitors, an effect commensurate with its enhanced biochemical potency. Moreover, the favorable metabolic stability, oral bioavailability, and pharmacokinetic properties of BMN 673 suggest that it is a useful addition to existing targeted agents in oncology.

Results

BMN 673 potently and selectively inhibits PARP1/2

Through a medicinal chemistry approach (Wang and colleagues, manuscript in preparation), we designed a series of drug-like small molecules that were able to inhibit the catalytic activity of PARP1. One compound, LT-00628 (Fig. 1A), showed a PARP1 IC_{50} of 1.82 nmol/L. LT-00628 contains two chiral centers and comprises a racemate that in theory consists of four isomers: L/R, R/L, L/L, and R/R. Chiral separation of LT-00628 indicated that LT-00628 is primarily made of *trans* isomers (L/R and R/L) with negligible amount of *cis* isomers. The *trans* isomers were obtained with chiral purity of greater than 97%. The absolute stereochemistry of BMN 673 was confirmed by single-crystal X-ray diffraction analysis (unpublished data). We found one of the *trans* isomers, LT-00673, to be highly potent with average PARP1 IC_{50} of 0.57 nmol/L (Fig. 1A). The other *trans* isomer, LT-00674, was relatively inactive (IC_{50} against PARP1 >100 nmol/L). As a residual amount of LT-00673 remained in LT-00674 (up to 0.8%), it was

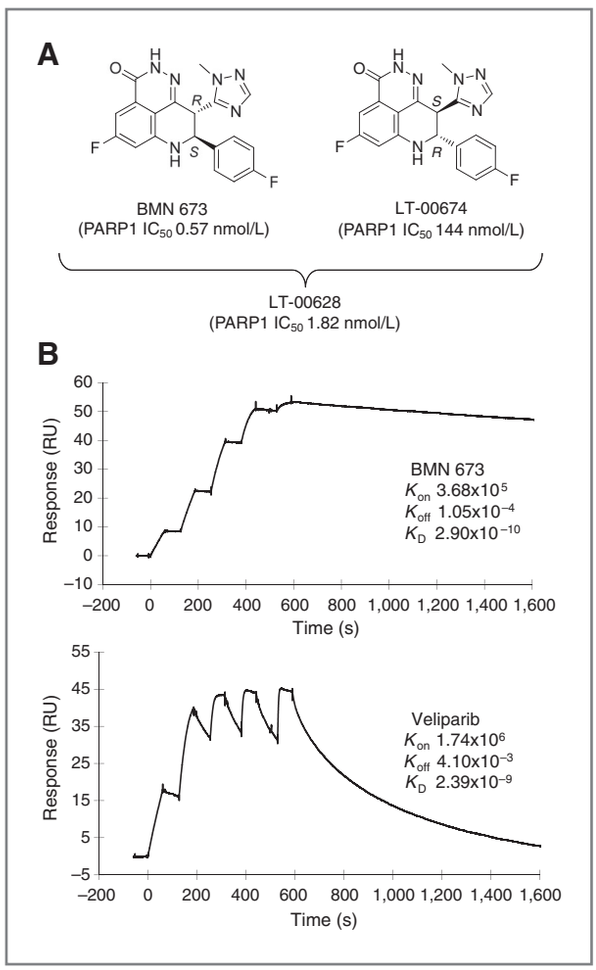

Figure 1. BMN 673 is a potent PARP inhibitor. A, structure and PARP1 IC_{50} of BMN 673, its corresponding isomer LT-00674, and the racemic mixture LT-00628. B, Biacore T200 sensorgrams of BMN 673 and veliparib binding to immobilized rhPARP1. Top, BMN 673 binding sensorgram; bottom, veliparib. Each compound was injected at increasing concentrations (12.5, 25, 50, 100, and 200 nmol/L; 60 s/injection) over a chip surface that was precoated with recombinant PARP1. The on-rates, off-rates, and K_D were determined as described in Materials and Methods.

Table 1. Summary of BMN 673 *in vitro* activities

	PARP1 enzyme inhibition IC_{50}, nmol/L	Cellular PAR synthesis EC_{50}, nmol/L	Capan-1 cytotoxicity IC_{50}, nmol/L	Temozolomide potentiation GI_{50}, nmol/L
Veliparib	4.73	5.9	>10,000	6,203
Rucaparib	1.98	4.7	609	144
Olaparib	1.94	3.6	259	237
LT-00628	1.82	4.5	8	5
BMN 673	0.57	2.5	5	3

NOTE: Activities of BMN 673, LT-00628, and three clinical PARP1/2 inhibitors veliparib, rucaparib, and olaparib were compared in four *in vitro* assays: (i) concentration for 50% inhibition in PARP1 enzyme assay (IC_{50}); (ii) concentration for 50% inhibition in cellular PAR synthesis assay in LoVo cells (EC_{50}); (iii) concentration for 50% Capan-1 cell survival reduction in single-agent cytotoxicity assay (IC_{50}); and (iv) concentration that, when combined with 200 μmol/L of temozolomide, resulted in 50% growth inhibition of LoVo cells in temozolomide potentiation assay (GI_{50}). Assay conditions are described in the Materials and Methods. Values are average data from three to four independent experiments.

possible that the weak activity shown by LT-00674 may have been caused by contamination with LT-00673. LT-00673 was later renamed as BMN 673 and its structure, (8*S*,9*R*)-5-fluoro-8-(4-fluorophenyl)-9-(1-methyl-1*H*-1,2,4-triazol-5-yl)-8,9-dihydro-2*H*-pyrido[4,3,2-de]phthalazin-3(7*H*)-one), is shown in Fig. 1A. In a side-by-side comparison, we found BMN 673 to be more potent than veliparib, rucaparib, and olaparib with IC_{50}s of 4.7, 2.0, and 1.9 nmol/L, respectively (Table 1). Even though the *cis* isomers were undetectable in the LT-00628 racemate, we designed a synthetic route to make the *cis* isomers alone; analysis of either *cis*-isomer showed these to be rather inactive as PARP inhibitors (Supplementary Table S1).

The kinetic characteristics of BMN 673 binding to PARP1 were assessed using Biacore T200. BMN 673 bound to PARP1 with an on-rate of 3.68×10^5 (1/ms), an off-rate of 1.05×10^{-4} (1/s), and a dissociation constant (K_D) of 2.90×10^{-10} mol/L (Fig. 1B, top). In contrast, veliparib under the same conditions displayed an on-rate of 1.74×10^6 (1/ms), an off-rate of 4.10×10^{-3} (1/s), and a K_D of 2.39×10^{-9} mol/L (Fig. 1B, bottom), suggesting BMN 673 to have a dissociation rate that is nearly 40 times slower than that of veliparib.

Most PARP1 inhibitors are known to also inhibit the homologous enzyme PARP2 due to the sequence similarity of PARP1 and -2 catalytic domains (14). We found that BMN 673 inhibited PARP1 and -2 to a similar extent, with K_i of 1.20 and 0.85 nmol/L, respectively. PARP1 and -2 are nuclear enzymes that synthesize PAR chains on target proteins as a form of posttranslational modification. To assess the ability of BMN 673 to inhibit intracellular PARP activity, we exposed LoVo cells to hydrogen peroxide (H_2O_2) to induce PAR synthesis and examined the ability of BMN 673 to inhibit PAR formation. Under these conditions, BMN 673 inhibited intracellular PAR formation with an IC_{50} of 2.5 nmol/L and was modestly more potent than veliparib, rucaparib, and olaparib, which had cellular PAR formation IC_{50}s of 5.9, 4.7, and 3.6 nmol/L, respectively (Table 1).

Several assays were used to examine the inhibition specificity of BMN 673. We first assessed the effect of BMN 673 on poly (ADP-ribose) glycohydrolase (PARG), a protein that is structurally related to PARP1/2. PARG degrades PAR modifications on proteins and in doing so can counter the effects of PARP1/2 signaling (15). Although BMN 673 profoundly inhibited PARP1/2, it had no effect on PARG activity at concentrations up to 1 μmol/L (data not shown). To identify other potential off-target activities, we screened BMN 673 against two commercially available protein panels, both from MDS Pharma: the Hit Profiling Screen Panel and the Adverse Reaction Enzyme Panel. At a 10 μmol/L concentration, BMN 673 did not have significant interaction, either inhibitory or stimulatory, with any of the receptors, ion channels, or enzymes assayed (data not shown). The effect of BMN 673 on the potassium ion channel hERG (the human Ether-à-*go-go*-Related Gene protein) was determined *in vitro*, with no significant inhibition observed at BMN 673 concentrations as high as 100 μmol/L, suggesting that BMN 673 is unlikely to cause clinical cardiac QTc elongation.

Identification of genetic determinants of BMN 673 sensitivity

Previous work has shown that PARP1/2 inhibitors selectively inhibit tumor cells with genetic defects that abrogate homologous recombination–mediated DSBR (6, 7, 16). To rapidly identify genetic determinants of BMN 673 sensitivity in an unbiased fashion, we conducted a series of parallel RNA interference drug sensitization screens (17) and compared the genetic sensitization profile of BMN 673 (i.e., the list of genes that modulated BMN 673 response) with those for three earlier generation clinical PARP1/2 inhibitors–olaparib, rucaparib, and veliparib. To do this, we used a siRNA library targeting 960 genes, encompassing kinases and kinase-related genes (17) as well as a series of tumor suppressors and DNA repair proteins (Supplementary Table S2). We used a moderately PARP inhibitor-resistant breast

tumor cell line (CAL51) previously used in similar studies (17) and screened each drug at a concentration required to elicit a 20% reduction in cell survival (surviving fraction 80, SF_{80}) so as to maximize the potential for identifying PARP1/2 inhibitor sensitization effects (17, 18). We did note that for BMN 673, SF_{80} in CAL51 was achieved at 12.5 nmol/L, compared with the micromolar concentrations of veliparib, rucaparib, or olaparib required to reach this level of cell inhibition. The effect of each siRNA on drug sensitization was quantified by the calculation of a drug effect *Z* score, with siRNAs returning drug effect *Z* scores of <-2 being considered significant sensitization effects (17).

The siRNAs that significantly sensitized tumor cells to BMN 673 are shown in Supplementary Table S3. This analysis revealed that the most profound effects on BMN 673 sensitivity were caused by siRNAs targeting genes involved in homologous recombination/DSBR including *BRCA2*, *BRCA1*, *SHFM1* (aka *DSS1*), *PNKP*, *PALB2*, *ATM*, *ATR*, *CHEK1*, *FANCM*, *FANCA*, etc. (Fig. 2A and Supplementary Table S3 genes highlighted in bold text). This observation suggested that homologous recombination/DSBR defects caused by any one of a number of genes caused cellular sensitivity to BMN 673, as is the case for other PARP1/2 inhibitors. To assess whether the overall genetic sensitization profile for BMN 673 was different from that of earlier generation PARP1/2 inhibitors, we compared the drug effect *Z* scores for all 960 genes from the BMN 673 screen to those derived from the other PARP1/2 inhibitor screens. The genetic sensitization profile for BMN 673 was not significantly different than the profiles generated by olaparib, rucaparib, or veliparib (Supplementary Table S4). These findings, collected in a relatively unbiased fashion, suggested that BMN 673 had the potential to target cells with defects in any one of a number of homologous recombination/DSBR genes.

BMN 673 targets tumor cells with defects in homologous recombination

Although siRNA screens are a rapid and useful means of identifying multiple genetic determinants of drug sensitivity in an unbiased fashion, and in this case confirmed that a number of different homologous recombination/DSBR genes modulated the response to BMN 673, the variable extent and stability of gene silencing achieved by siRNA often limits their ability to accurately define the scale of sensitization caused by a particular gene–drug combination. To formally assess the scale of selectivity of BMN 673 for tumor cells with homologous recombination gene defects, we measured the ability of BMN 673 to inhibit cells with either *BRCA1* or *BRCA2* gene mutations. We first tested the inhibitory effects of BMN 673 and other clinical PARP1/2 inhibitors in a panel of human tumor cell lines (Table 2). Models such as SW620 and MDA-MB-231 that do not have *BRCA* gene mutations or homologous recombination/DSBR defects were relatively resistant to BMN 673 with SF_{50}s of 0.13 and 1.85 μmol/L, respectively (Table 2). Likewise, nontransformed MRC-5 cells were also resistant to BMN 673. In contrast, tumor models that were either BRCA1-deficient (MX-1 and SUM149) or BRCA2-deficient (Capan-1) were profoundly sensitive to BMN 673 (Table 2). PTEN deficiency (for example caused by N-terminal *PTEN* truncating mutations) has previously been shown to cause a defect in homologous recombination and sensitivity to other PARP1/2 inhibitors (19). We found BMN 673 to be

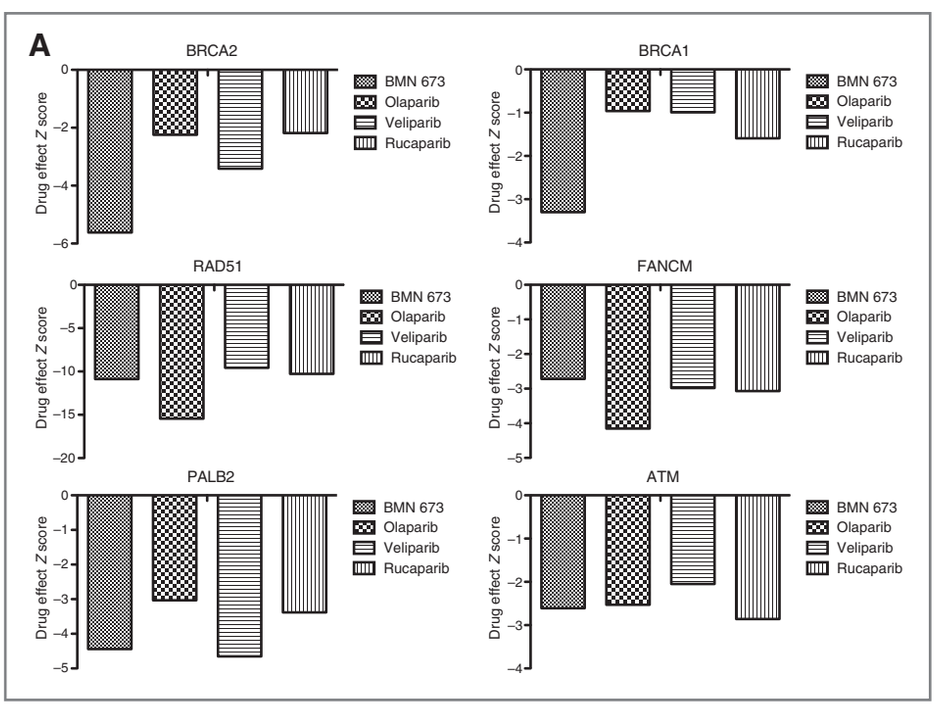

Figure 2. A, siRNAs targeting homologous recombination genes sensitize to PARP1/2 inhibitors. CAL51 cells were transfected with a library of siRNAs and treated with BMN 673, olaparib, veliparib, or rucaparib. Each drug was used at its respective SF_{80} concentration. The effect of each siRNA on drug sensitization was quantified by the calculation of a drug effect *Z* score. Out of 960 genes, those involved in homologous recombination–mediated DNA repair were a prominent feature of the sensitivity profile of all PARP1/2 inhibitors. Drug effect *Z* scores for *BRCA1 BRCA2*, *ATM*, *FANCM*, *RAD51*, and *PALB2* are shown here. (*Continued on the following page*.)

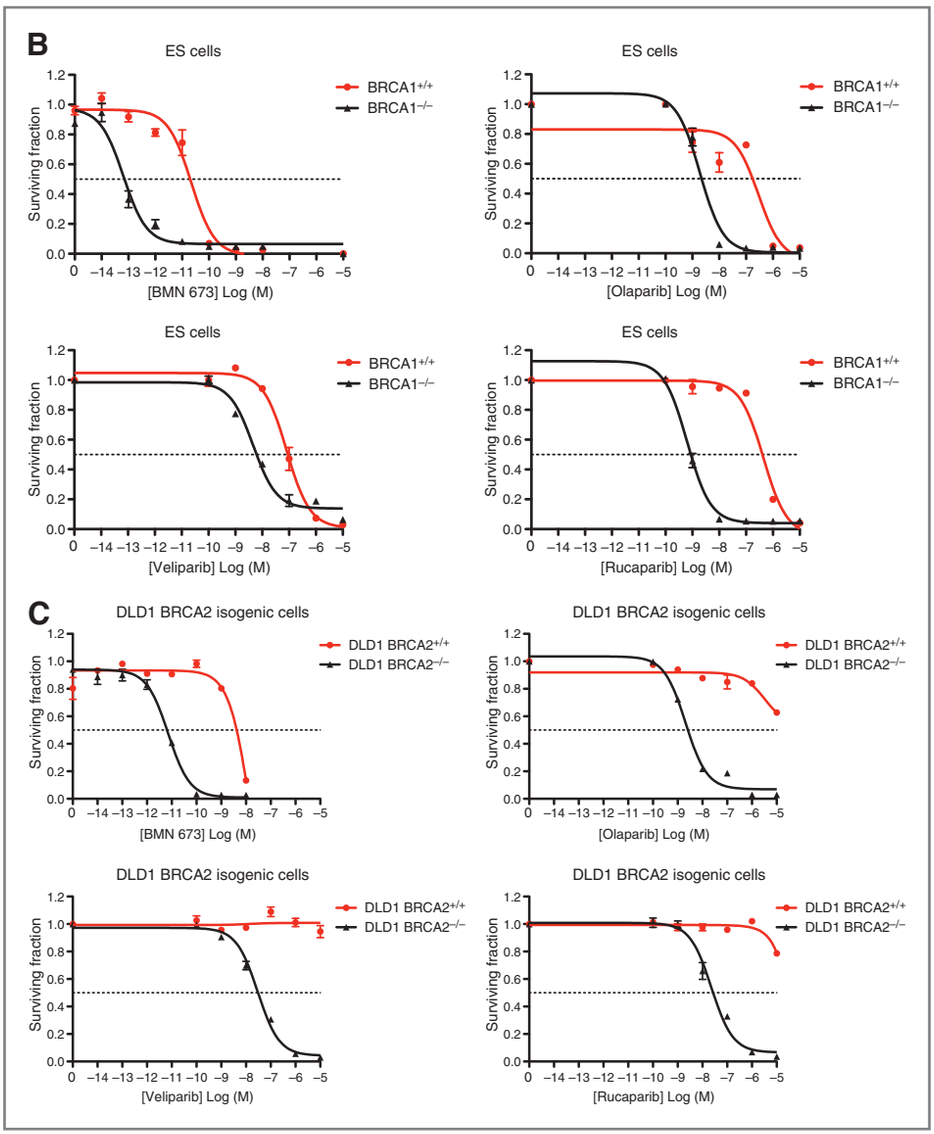

Figure 2. (*Continued.*) B and C, BMN 673 is selectively toxic to BRCA1- or BRCA2-deficient cells. Dose–response curves from clonogenic survival assays in a variety of isogenic models are shown. The response of BRCA1-deficient and -proficient embryonic stem (ES) cells (generated by gene targeting) are shown as are the responses in human DLD1 tumor cell lines with *BRCA2* gene-targeted alleles. Cells were exposed to different PARP1/2 inhibitors as shown for 10 to 14 days, after which surviving colonies were counted and surviving fractions calculated by normalizing surviving colony numbers to colony numbers in control (vehicle-treated) cells.

highly potent in inhibiting human tumor cells with PTEN deficiency (Table 2). For example, the SF_{50} values for BMN 673 in the PTEN-null models MDA-MB-468, LNCap, and PC-3 were 6, 3, and 4 nmol/L, respectively, values comparable with SF_{50}s in BRCA deficient models.

It was notable that compared with other clinical PARP1/2 inhibitors, BMN 673 was at least 18-fold more potent in BRCA-deficient tumor cells. In the *BRCA1*-mutant, triple-negative [estrogen receptor (ER), progesterone receptor (PR), and HER2 negative) breast tumor cell line model SUM149, BMN 673 delivered a SF_{50} of 8×10^{-12} mol/L, 1×10^{5}–fold lower than that of veliparib (SF_{50} = 0.8 μmol/L) and 922 and 231 times lower than that of rucaparib and olaparib, respectively (Table 2). In contrast, the differences in PARP1/2 inhibitor SF_{50} between different PARP1/2 inhibitors in cells without homologous recombination/DSBR defects was significantly less (Table 2). To confirm the BRCA selectivity of BMN 673, we also assessed cell growth inhibition in isogenic models of BRCA deficiency, namely mouse embryonic stem cells carrying *BRCA1* gene defects (20) as well as human DLD1 tumor cells carrying homozygous *BRCA2* gene knockout (21). In both model systems, BMN 673 selectivity inhibited BRCA-deficient cells and delivered a therapeutic window between BRCA-proficient and -deficient models at much reduced concentrations when compared with veliparib, rucaparib, or olaparib (Fig. 2B and C).

Compared with other PARP1/2 inhibitors, BMN 673 is about 3- to 8-fold more potent at inhibiting PARP1/2 enzymatic activities, but has a much greater potency advantage in inhibiting BRCA-deficient cells when used as a single agent (Table 2 and Fig. 2). This raised the possibility that the ability of BMN 673 to inhibit these

Table 2. Selective killing of tumor cells with BRCA1, BRCA2, or PTEN mutations

	SF_{50}, μmol/L								
	MX-1 (BRCA1 deficient)	SUM149 (BRCA1 deficient)	Capan-1 (BRCA2 deficient)	MB-468 (PTEN deficient)	LNCap (PTEN deficient)	PC-3 (PTEN deficient)	SW620	MDA-MB-231	MRC-5 (normal)
Veliparib	ND	0.818	>10	ND	ND	ND	ND	ND	>10
Rucaparib	0.0053	0.0079	0.609	0.220	0.737	0.293	ND	5.53	8.53
Olaparib	0.0232	0.0198	0.259	0.368	0.589	0.787	ND	6.41	5.83
BMN 673	0.0003	8.57E-6	0.005	0.006	0.003	0.004	0.13	1.85	0.31

NOTE: Cultured human tumor cell lines were treated with veliparib, rucaparib, olaparib, or BMN 673, and tumor-killing effects were assessed either by colony formation assays (SUM149) or by two-dimensional cytotoxicity assays (all other cell lines). Survival curves were plotted and the IC_{50} was calculated as the concentration required to kill 50% of the cells. Known deficiency of homologous recombination DNA repair genes is indicated in parenthesis. Cells with *BRCA1*/*BRCA2* mutations or PTEN deficiency were more sensitive to all PARP inhibitors than cells lacking these mutations.
Abbreviation: ND, not determined.

cells might be partially due to activities that are unrelated to PARP1/2 inhibition. To investigate this possibility, we compared the *in vitro* activities of BMN 673 and its *trans* isomer LT-00674, which, despite the structural similarity, had a greatly reduced PARP1/2 inhibitory activity when compared with BMN 673. There was a strikingly tight correlation between PARP1 enzyme inhibition and the ability to inhibit the BRCA2-deficient cancer cell line Capan-1 as well as the ability to sensitize tumor cells to temozolomide, another well-established property of PARP1/2 inhibitors (Supplementary Table S5). The correlation of the chiral selectivity strongly suggested that the potent inhibition of cancer cells is a direct effect of BMN 673 PARP inhibition.

BMN 673 induces DNA damage at picomolar concentrations

One working hypothesis that could explain the homologous recombination-selectivity of PARP1/2 inhibitors centers on their ability to cause a DNA lesion or lesions that inhibit the normal function of the replication fork (22). The frequency of stalled and damaged replication forks caused by PARP1/2 inhibitors can be monitored by estimating the formation of nuclear γ-H2AX foci (6, 23). We assessed the ability of BMN 673 to induce nuclear γ-H2AX foci formation, as measured by immunofluorescence and confocal microscopic imaging. We found that BMN 673 induced nuclear γ-H2AX foci at concentrations as low as 100 pmol/L (Supplementary Fig. S1). In contrast, 100 nmol/L of olaparib was required to elicit a similar γ-H2AX response, suggesting that the increased intrinsic potency of BMN 673 also resulted in an increased ability to elicit a DNA response biomarker.

Metabolism and pharmacokinetic properties of BMN 673

One of the objectives of our PARP inhibitor discovery program was to improve metabolic stability, pharmacokinetic properties, and oral bioavailability over existing PARP1/2 inhibitors. *In vitro* metabolism studies of BMN 673 in liver microsomes from rats, dogs, and humans showed that BMN 673 had excellent liver microsome stability; more than 90% of BMN 673 remained after 2 hours of incubation at 1 μmol/L concentration (Supplementary Table S6). In rat pharmacokinetic studies, BMN 673 showed oral bioavailability of more than 40% when dosed in 0.5% carboxylmethyl cellulose, and pharmacokinetic properties that would predict a human half-life that is sufficient to support a regimen of once daily administration (manuscript in preparation). *In vitro* studies assessing the potential for inhibition of human cytochrome P450 enzymes (CYP450s) showed that at concentrations up to 10 μmol/L, BMN 673 did not inhibit any of the five major human hepatic CYP450 enzymes (CYP1A2, 2C9, 2C19, 2D6, and 3A4; data not shown). Overall, BMN 673 showed excellent metabolic stability, oral bioavailability, and pharmacokinetic properties.

Antitumor effect of BMN 673 oral administration in xenograft tumor models

To assess the *in vivo* antitumor effects of BMN 673, when used as a single agent, we treated nude mice bearing established subcutaneous MX-1 tumor xenografts with BMN 673. MX-1 is a human mammary carcinoma cell line that harbors *BRCA1* deletion events and is BRCA1 deficient (24). Oral administration of BMN 673 for 28 days (once a day dose of 0.33 mg/kg) significantly inhibited the growth of MX-1 xenografts in mice, with 4 of 6 mice achieving a complete response (CR; tumor impalpable; Fig. 3A). At the lower dose of 0.1 mg/kg, oral BMN 673 only had a small effect on tumor growth after extended treatment (>21 days; Fig. 3A), but was still more effective than olaparib dosed orally at 100 mg/kg once daily. BMN 673 at these doses (0.33 and 0.1 mg/kg) was well tolerated, with no animal lethality or significant

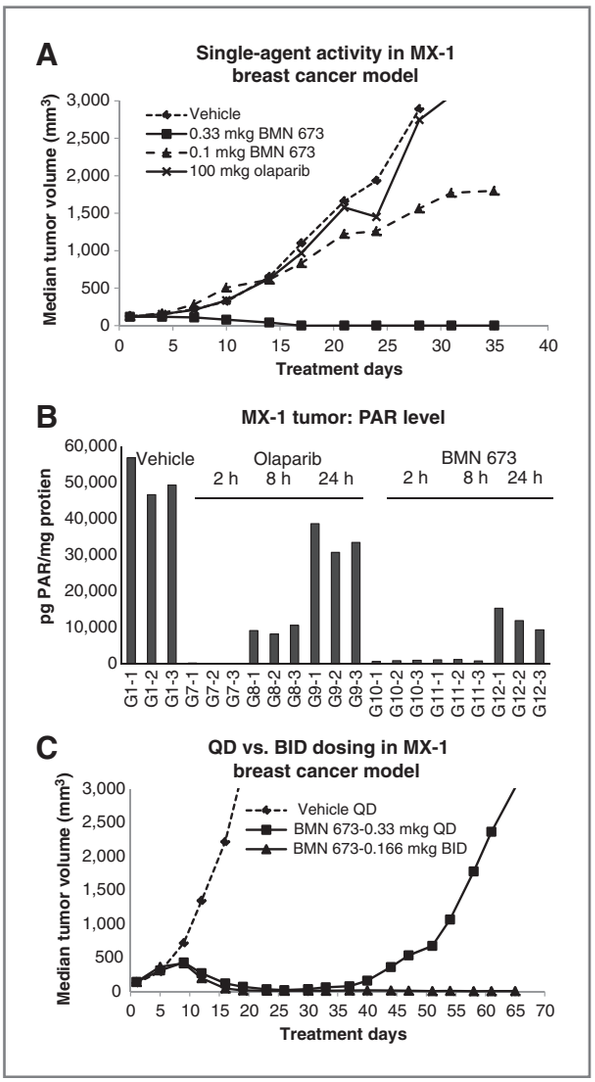

Figure 3. BMN 673 exhibits antitumor activity against a BRCA-mutant tumor model in mice. A, MX-1 human mammary xenografts were inoculated subcutaneously in female athymic nu/nu mice. When tumors reached an average volume of approximately 150 mm^3 (range, 100–196 mm^3), mice were randomized into various treatment groups, and were treated orally, once daily for 28 consecutive days, with BMN 673 (0.33 or 0.1 mg/kg/d), olaparib (100 mg/kg/d), or empty vehicle. Median tumor volume was plotted against days of treatment (first day of treatment is defined at day 1). B, inhibition of PARP activity by a single oral dose of BMN 673 (1 mg/kg) was shown *ex vivo* by measuring MX-1 tumor PAR levels at 2 and 8 hours and the inhibition was partially recovered 24 hours after dosing. Intratumoral PARP inhibition was also observed with olaparib at 100 mg/kg oral administration, but the effect was much shorter. Each bar represents an individual tumor from an individual animal. C, BMN 673 is more effective in mouse xenograft models with 0.165 mg/kg/dose twice a day (BID) dosing than 0.33 mg/kg/dose once a day (QD) dosing. In the MX-1 model, not only did all 6 mice treated with 0.165 mg/kg/dose 2×/day regimen reached CR, but also none of the mice had tumor regrowth until the end of the study, 8 weeks after BMN 673 dosing stopped. Median tumor volume was plotted against days of treatment (first day of treatment is defined at day 1).

weight loss observed after 28 consecutive, once daily, oral doses.

To assess the *in vivo* pharmacodynamics of BMN 673 (PARP inhibition), we gave MX-1 xenograft-bearing mice a single oral administration of 1 mg/kg BMN 673. Tumors were harvested at 2, 8, and 24 hours postdrug dosing, and intratumor PAR levels were determined using an anti-PAR ELISA. BMN 673 treatment drastically decreased intratumoral PAR levels at 2 and 8 hours following drug administration. Partial recovery of basal PAR levels was observed at 24 hours after dosing (Fig. 3B), an effect probably due to the clearance of BMN 673. In comparison, a single oral administration of olaparib at 100 mg/kg produced a significant decrease of intratumoral PAR level at 2-hour postdosing, with partial recovery at 8 hours and complete recovery at 24 hours.

Subsequent studies that were designed to assess various intermittent dosing schedules of BMN 673 showed little benefit in terms of tumor growth delay (data not shown), suggesting that continuous suppression of PARP might be required for a therapeutic effect. As PAR levels partially recovered in mouse xenograft tumors between 8 and 24 hours postadministration of BMN 673 (Fig. 3B), we reasoned that twice a day dosing might be more effective than a once a day dosing regimen. To test this hypothesis, we compared the antitumor effect of administration of BMN 673 at 0.33 mg/kg/dose once a day for 28 days versus 0.165 mg/kg/dose twice a day for 28 days in MX-1 tumor-bearing mice. The results of these studies indicated that both once a day and twice a day dosing regimens inhibited MX-1 tumor growth with significant tumor regression (Fig. 3C). Once a day treatment generated four CRs out of 6 animals, consistent with the previous experiment. However, while tumors in the once a day–treated cohort did eventually reestablish after BMN 673 treatment ceased, the twice a day for 28 days treatment schedule resulted in 6 of 6 CRs with no reestablishment of tumor until the end of the study, 8 weeks after BMN 673 dosing ceased (Fig. 3C). One of six mice treated with twice a day had significant weight loss (>20%) and was sacrificed on day 53. All other animals in the study tolerated the treatment well. Taken together with the results from the *in vivo* PAR inhibition study (Fig. 3B), these results suggested that continuous suppression of PARP1/2 is required for maximum antitumor effect in the context of a single-agent application, and that in mice, twice a day dosing of BMN 673 was necessary to achieve optimal therapeutic effect, perhaps by continuously suppressing PARP activity. It should be noted that the half-life of BMN 673 in human is expected to be much longer (due to slower metabolism) than in mice. Therefore, we anticipate that once a day dosing will be sufficient in human patients to continuously suppress PARP and show anticancer effect. The effectiveness of once a day oral dosing in human has been validated in phase I clinical trials of BMN 673 (data to be published in ASCO 2013, Chicago).

The antitumor effect of BMN 673 on growth of PTEN-null tumors was also examined *in vivo* (Supplementary

Fig. S2). Two PTEN-null cell lines were established as subcutaneous xenograft models in nude mice, and treated with 0.33 mg/kg BMN 673 (oral, once a day for 28 days). Both tumor models responded well to BMN 673 treatment, resulting in tumor growth delay of 15.9 days (MDA-MB-468) and 22.8 days (LNCap) when compared with the vehicle-treated control cohort. In a separate study, we showed that treatment with BMN 673 at 0.165 mg/kg/dose twice a day for 28 days was slightly more effective than 0.33 mg/kg/dose once a day for 28 days in the MDA-MB-468 xenograft model, consistent with the MX-1 tumor study results described earlier (Supplementary Fig. S3).

BMN 673 sensitizes tumor cells to DNA-damaging chemotherapies

The chemosensitizing property of PARP1/2 inhibitors has been well documented (25). One of the most robust chemopotentiation effects involves the combination of temozolomide with PARP1/2 inhibitors (26–29). To investigate whether BMN 673 shared this characteristic, we tested its ability to potentiate the cytotoxic effect of temozolomide using an *in vitro* assay. We found that single-agent temozolomide exposure (200 μmol/L) resulted in approximately 15% cell growth inhibition after a 5-day treatment in LoVo tumor cells (Fig. 4A). Combining BMN 673 with 200 μmol/L temozolomide resulted in a significant potentiation of temozolomide cytotoxicity (Fig. 4A and Table 1). We also examined the effect of BMN 673 on SN-38, active metabolite of the DNA topoisomerase I inhibitor irinotecan. BMN 673 potentiated the cytotoxic effect of SN38 in MX-1 cells *in vitro* in a dose-dependent manner (Fig. 4B).

We observed a clearly additive effect of combining BMN 673 with platinum drugs *in vitro* (data not shown). The ability of BMN 673 to potentiate platinum drugs *in vivo* was also readily shown. We first examined the effect of BMN 673 on cisplatin-induced antitumor effect. Growth of MX-1 tumor xenografts implanted subcutaneously in female athymic mice was significantly inhibited in a dose-dependent manner when animals were treated with BMN 673 in combination with a 6 mg/kg intraperitoneal injection of cisplatin (Fig. 4C). However, we did note that the combination regimens involving cisplatin resulted in moderate body weight loss. Maximum average weight loss of 11%, 6%, 5%, and 3% were observed for groups that contained BMN 673 doses of 1, 0.33, 0.1, and 0.033 mg/kg, respectively. In the same experiment, animals that were treated with cisplatin alone had maximum average body weight loss of 3%. One animal died in the BMN 673 1 mg/kg plus cisplatin group on day 20, whereas most animals recovered their body weight after treatment terminated. Olaparib at 100 mg/kg also showed activity in this treatment regimen, with a maximum body weight loss of 3%. In a separate study, BMN 673 showed significant potentiation of carboplatin antitumor effect *in vivo* (Fig. 4D). No animal lethality or significant body weight loss was observed.

Discussion

Here, we describe a novel, potent, and selective PARP1/2 inhibitor BMN 673. Like other PARP1/2 inhibitors, BMN 673 is selective for tumor cells with defects in homologous recombination, as shown by a siRNA drug sensitivity profile that encompasses genes involved in homologous recombination/DSBR and by assessment in isogenic and nonisogenic models of BRCA1, BRCA2, and PTEN deficiency. These effects were also observed *in vivo* in mouse xenograft models where tumors with either *BRCA1* or *PTEN* defects showed significant tumor growth delay after oral administration of BMN 673. Furthermore, the antitumor effects of temozolomide, cisplatin, and carboplatin were all potentiated by BMN 673. These therapeutic effects were achieved with tolerable toxicity, evidence of PAR inhibition *in vivo* in animal tumor models, and favorable pharmacokinetic properties that allow once a day oral dosing in human patients.

With K_i of 1.2 and 0.9 nmol/L against PARP1 and -2, respectively, BMN 673 is the most potent PARP inhibitor reported to date. Still, we were initially surprised by the much greater cytotoxicity in homologous recombination–deficient cells compared with other PARP1/2 inhibitors that have apparently comparable potency against PARP catalytic activity. We initially suspected that BMN 673 might have activity other than PARP1 and -2 inhibition, and that this activity may be responsible for or contributing to the increase in tumor cell inhibition. However, chiral selectivity (Supplementary Table S5) shown by the BMN 673/LT-00674 isomer pair strongly suggests that its remarkable cytotoxic properties in homologous recombination/DSBR–deficient cells is very likely a direct result of its ability to inhibit PARP1/2.

BMN 673 showed a notable preference for tumor cells harboring BRCA1, BRCA2, or PTEN dysfunction. Although other PARP inhibitors such as veliparib, rucaparib, and olaparib showed selectivity in homologous recombination–deficient cells versus homologous recombination–proficient cells when used at micromolar concentrations, the selectivity margin of BMN 673 could be achieved with nanomolar or even picomolar concentrations in isogenic models. In some nonisogenic systems (Table 2), the therapeutic window between BRCA-deficient and -proficient models was enhanced compared with other clinical PARP1/2 inhibitors (Fig. 2). The siRNA screen also confirmed that, out of 960 genes tested, the most profound effects on BMN 673 sensitivity were caused by siRNAs targeting genes involved in homologous recombination/DSBR. Although a two-sided *t* test did not show statistically significant differences between BMN 673 and other PARP inhibitors in their sensitization profiles (Supplementary Table S4), it is intriguing to note that silencing of DSBR genes *BRCA1*, *BRCA2*, *PNKP*, *ATR*, *CHEK1*, and *PALB2* resulted in sensitization for BMN 673 (Supplementary Table S3) at a low nmol/L dose of the drug. This may generate a large therapeutic window for BMN 673, making it potentially more efficacious while maintaining manageable toxicity.

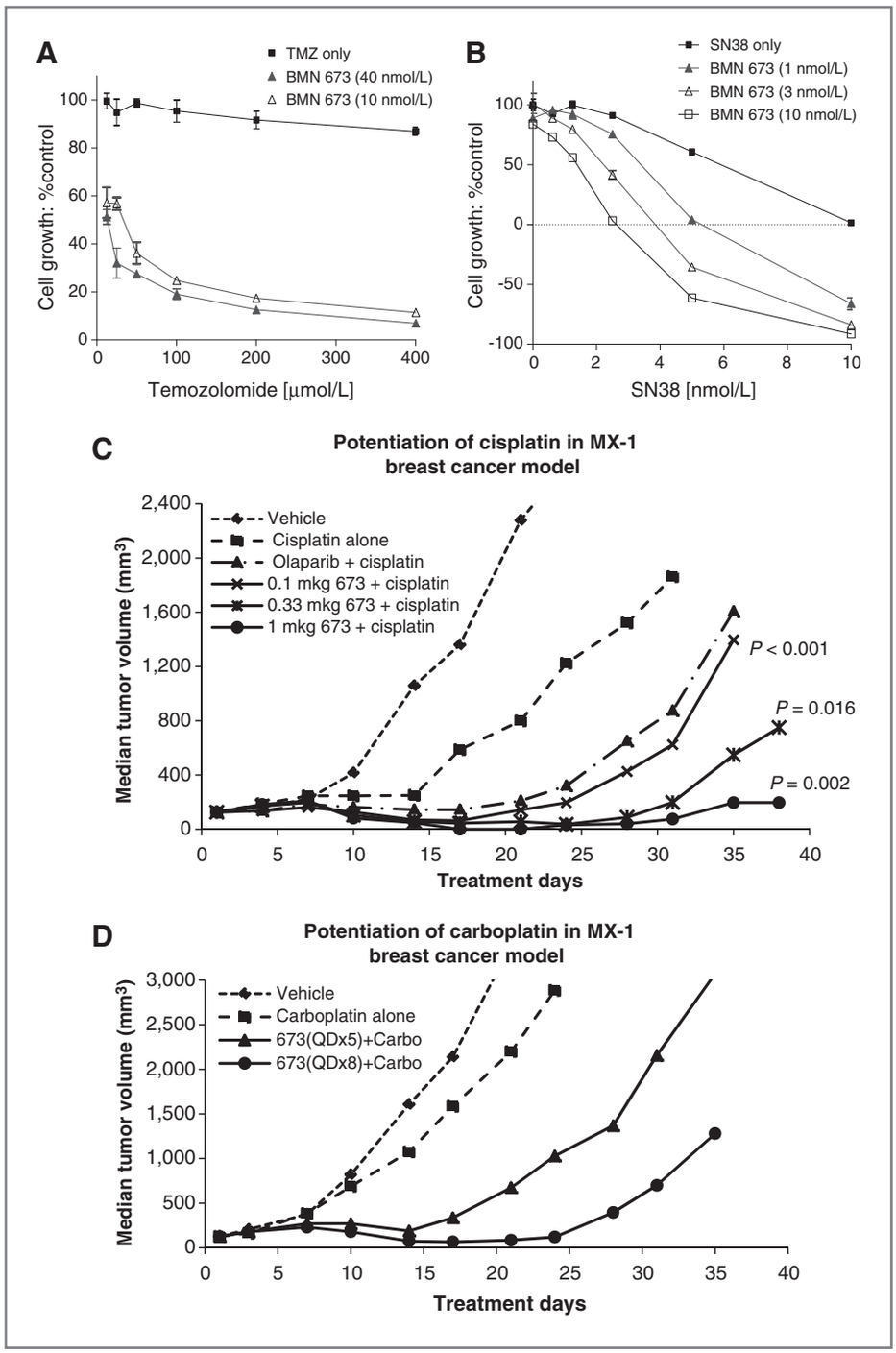

Figure 4. BMN 673 potentiates the effects of DNA-damaging cytotoxic agents. A, LoVo cells were treated with BMN 673 and temozolomide (TMZ) either alone or in combination for 5 days. Surviving fraction was determined using CellTiter-Glo assay. BMN 673 significantly increased the cytotoxicity of temozolomide in LoVo cells. B, BMN 673 sensitized MX-1 cells to SN-38 cytotoxicity in a dose-dependent fashion. C, nude mice carrying MX-1 tumor xenografts were treated with oral administration of BMN 673, olaparib, or vehicle once a day (QD) from day 1 to 8. Cisplatin was dosed intraperitoneally at 6 mg/kg on the third day of PARP inhibitor treatment. Although 0.1, 0.33, and 1 mg/kg of BMN 673 showed dose-dependent sensitization of the cisplatin, 100 mg/kg olaparib showed a sensitizing effect that is equivalent to the lowest dose of BMN 673. D, Once a day dosing of BMN 673 for 8 days potentiated carboplatin more than 5 daily dosing, which in turn generated tumor growth inhibition more than carboplatin alone. BMN 673 was dosed orally, once a day for either 5 or 8 days starting on day 1, at a dosage level of 0.33 mg/kg. Carboplatin at a dosage of 35 mg/kg or its vehicle (saline) for the control group was administered intraperitoneally on day 1, half an hour after BMN 673 administration. Median tumor volume was plotted against days of treatment (first day of treatment is defined at day 1).

PARP1/2 inhibitors are an exciting new class of anticancer agents that exploit the biologic concept of synthetic lethality as the basis for their antitumor selectivity (6, 7). However, the clinical use of PARP1/2 inhibitors is still in its infancy. Despite promising phase I and II trial results with olaparib, rucaparib, and niraparib (4, 8–11) further development has been slow with problems such as toxicity when combined with chemotherapeutic agents (30, 31), difficulty in defining suitable patient populations beyond those with *BRCA1* or *BRCA2* mutations (32), or formulation issues. However, given the effectiveness of PARP1/2 inhibitors in patients with germline *BRCA* mutations (8–10), this area is still ripe for further study and exploration. Two phase I clinical trials are currently ongoing for BMN 673 that are assessing its safety, pharmacokinetic, and pharmacodynamic properties and preliminary efficacy in human patients. In January 2011,

a first in human, single-arm, open-label study in patients with advanced tumors with DNA-repair pathway deficiencies was initiated followed by a two-arm, open-label study in patients with advanced hematologic malignancies, which was started in June 2011. The discovery and characterization of BMN 673, as a potent, selective, orally bioavailable PARP1/2 inhibitor and its advancement into phase I studies thus provides a welcome addition to this field.

Materials and Methods

Drugs and cell lines

Synthesis of LT-00628, BMN 673, LT-00674, and LT-00878 is described elsewhere (33, 34). Olaparib, rucaparib, and veliparib used in this study were either synthesized as previously described (35–37) or obtained from Selleck Chemicals. Drug stock solutions were prepared in dimethyl sulfoxide (DMSO) and stored in aliquots at −20°C. Drugs (alone or in combination) were added to cell cultures so that final DMSO concentrations were constant at 1% (v/v). MX-1 was obtained from National Cancer Institute (Bethesda, MD). All other cell lines were obtained from American Type Culture Collection and maintained as exponentially growing monolayers according to the supplier's instructions.

PARP enzyme assays

The ability of a test compound to inhibit PARP1 enzyme activity was assessed using Trevigen's PARP Assay Kit (Trevigen CAT#4676-096-K) following the manufacturer's instruction. IC_{50} values were calculated using GraphPad Prism5 software. For PARP inhibitor K_i determination, enzyme assays were conducted in 96-well FlashPlate (PerkinElmer) with 0.5 U PARP1 enzyme (Trevigen; Cat#4667-250-EB), 0.25× activated DNA (Trevigen), 0.2 μCi [^{3}H] NAD (PerkinElmer; Cat#NET443H250UC), and 5 μmol/L cold NAD (Sigma) in a final volume of 50 μL reaction buffer containing 10% glycerol (v/v), 25 mmol/L HEPES, 12.5 mmol/L $MgCl_2$, 50 mmol/L KCl, 1 mmol/L dithiothreitol (DTT), and 0.01% NP-40 (v/v), pH 7.6. Reactions were initiated by adding NAD to the PARP reaction mixture with or without inhibitors and incubated for 1 minute at room temperature. Fifty microliter of ice-cold 20% trichloroacetic acid (TCA) was then added to each well to stop the reaction. The plate was sealed and shaken for a further 120 minutes at room temperature, followed by centrifugation. Radioactive signal bound to the FlashPlate was determined using TopCount. PARP1 K_m was determined using Michaelis–Menten equation from various substrate concentrations (1–100 μmol/L NAD). Compound K_i was calculated from enzyme inhibition curve according to the formula: $K_i = IC_{50}/[1+(\text{substrate})/K_m]$. K_m for PARP2 enzyme and compound K_i were determined with the same assay protocol except 30 ng PARP2 (BPS Bioscience; Cat#80502), 0.25× activated DNA, 0.2 μCi [^{3}H] NAD, and 20 μmol/L cold NAD were used in the reaction for 30 minutes at room temperature.

Biacore-binding assay

Recombinant human PARP1 (rhPARP1) catalytic domain (residues 662–1011) with N-terminal 6× His-tag was generated in house at BioMarin Pharmaceutical Inc. and used in binding assay for PARP inhibitor interaction using Biacore T200 (GE Healthcare). rhPARP1 was immobilized on a CM5 sensor chip (GE Healthcare) by amine coupling method. Briefly, one flow cell of a CM5 chip was first activated by a 7-minute injection at 10 μL/min of freshly prepared 50 mmol/L N-hydroxysuccinimide (NHS): 200 mmol/L 1-ethyl-3-(3-dimethylaminopropyl)carbodiimide hydrochloride (EDC) (1:1; GE Healthcare) at rate of 10 μL/min. Then rhPARP1 (100 μg/mL, in 10 mmol/L MES pH 6.5) was injected onto the flow cell for 60-second at 10 μL/min. The remaining active coupling sites were blocked with a 7-minute injection of 1 mol/L ethanolamine at 10 μL/min. The immobilization buffer contains 10 mmol/L HEPES pH 7.4, 150 mmol/L NaCl, 0.05% Surfectant P20, 5 mmol/L $MgCl_2$, and 0.5 mmol/L TCEP [tris(2-carboxyethyl)phosphine]. The immobilization level was approximately 7,600 response unit (RU). For binding kinetics measurement, PARP inhibitors at increasing concentrations (12.5, 25, 50, 100, and 200 nmol/L) were injected over the chip surface for 60 seconds per injection. The exposure was followed by a dissociation phase of 3,600 seconds in running buffer (immobilization buffer + 1% DMSO) after the last injection. The flow rate was 50 μL/min. After sensorgrams were corrected for signals from a reference flow, kinetics was calculated with Biacore T200 evaluation software ver.1.0 (Biacore; GE Healthcare).

Intracellular PAR formation assay

Cellular PAR synthesis assay assesses the ability of a test compound to inhibit polymerization of PAR. LoVo human colorectal tumor cells grown in 96-well microtiter plates overnight were pretreated with increasing concentrations of PARP inhibitors for 30 minutes before H_2O_2 was added at a final concentration of 50 mmol/L. After a 5-minute treatment at room temperature, cells were fixed for 10 minutes with prechilled methanol/acetone (7:3) at −20°C. Fixed cells were incubated with anti-PAR monoclonal antibody (Trevigen) for 60 minutes, followed by incubation with fluorescein isothiocyanate (FITC)-coupled goat anti-mouse immunoglobulin G (IgG; diluted at 1:100) and 1 μg/mL 4′,6-diamidino-2-phenylindole (DAPI) for 60 minutes. FITC signal was normalized with DAPI signal, and EC_{50} values were calculated using GraphPad Prism.

siRNA screen

CAL51 cells plated in 96-well plates were transfected 24 hours later with siRNA (final concentration 100 nmol/L), using Oligofectamine (Invitrogen) as per the manufacturer's instructions. At 48 hours after transfection, three replica plates were treated with 0.01% (v/v) DMSO vehicle in media and three replica plates with each PARP1/2 inhibitor in media. Cell viability was assessed after 5 days of PARP1/2 inhibitor exposure using CellTiter-Glo Luminescent Cell Viability Assay (Promega) as per the manufacturer's instructions. Data from each screen were analyzed as described previously (18).

Colony formation survival assays

Colony formation assays were conducted as described previously (6). In brief, cells were seeded into 6-well plates at a concentration of 500 to 2,000 cells per well. After 24 hours, media was replaced with fresh media containing PARP1/2 inhibitor. This procedure was repeated twice weekly for 14 days, at which point colonies were fixed with TCA and stained with sulforhodamine B. Colonies were counted and surviving fractions calculated by normalizing colony counts to colony numbers in vehicle-treated wells. Survival curves were plotted using a four-parameter logistic regression curve fit.

Single-agent cytotoxicity and chemosensitization assays

In single-agent assays, cells are seeded in a density that allows linear growth for 10 to 12 days in 96-well plates (typically 500–3,000 cells/well). Cells were treated in their recommended growth media containing increasing concentrations of PARP inhibitors for 10 to 12 consecutive days (media changed with fresh compounds every 5 days). In chemosensitization assays, PARP inhibitors at various concentrations were either combined with 200 μmol/L temozolomide to treat LoVo cells or with SN-38 (0–10 nmol/L), an active metabolite of Irinotecan to treat MX-1 cells for 5 days. After treatments, cell survival was determined by CellTiter-Glo assay (Promega), expressed as relative to mock treatment control (0.1%–0.5% DMSO), and IC_{50} or GI_{50} values were calculated using GraphPad Prism5 software.

Confocal microscopy

Cells were seeded on coverslips placed in 6-well plates and after 24 hours treated with several concentrations of olaparib or BMN 673. Twenty-four hours after treatment, the cells were fixed in 10% formalin (3.7% PFA) for 1 hour. Cells were permeabilized with 0.2% Triton X-100 in PBS for 20 minutes, treated with 50 μL DNase I (Roche; diluted at 1:10 in PBS) for 1 hour at 37°C and then blocked with IFF (PBS + 1% BSA and 2% FBS followed by filter sterilization) for 1 hour. The coverslips were then incubated with rabbit anti-γ-H2Ax primary (Millipore) and mouse anti-RAD51 primary (Epitomics Lot YI031608C; both 1:1,000 in 50 μL immunofluorescent buffer (IFF)) overnight at 4°C. Next day, the cells were incubated with anti-mouse Alexa Fluor 546 secondary and anti-rabbit Alexa Fluor 488 secondary (both 1:1,000 in 50 μL IFF) for 1 hour. Cells were then washed in PBS containing DAPI 1:10,000 for 10 minutes and attached on glass plates using Vectashield and nail polish. A minimum of four pictures were made of each coverslip using the Leica confocal microscope, and cells were subsequently counted. At least 100 cells were assessed per coverslip, being positive for γ-H2Ax if they had more than 5 foci per nucleus. The percentage of positive cells was plotted.

Xenograft experiments

Female athymic nu/nu mice (8–10-week old) were used for all *in vivo* xenograft studies. Mice were quarantined for at least 1 week before experimental manipulation. Exponentially growing cells (LNcap and MDA-MB-468) or *in vivo* passaged tumor fragments (MX-1) were implanted subcutaneously at the right flank of nude mice. When tumors reached an average volume of approximately 150 mm^3, mice were randomized into various treatment groups (6–8 mice/group) in each study. Mice were visually observed daily and tumors were measured twice weekly by calliper to determine tumor volume using the formula $[\text{length}/2] \times [\text{width}^2]$. Group median tumor volume (mm^3) was graphed over time to monitor tumor growth. In single-agent studies, olaparib (100 mg/kg), BMN 673 (various doses as indicated), or vehicle (10% DMAc, 6% Solutol, and 84% PBS) was administered by oral gavage (*per os*), once daily or BMN 673 (0.165 mg/kg) twice daily for 28 consecutive days. Mice were continuously monitored for 10 more days after last day of dosing. In cisplatin combination study, BMN 673, olaparib, or vehicle was administered *per os* once daily for 8 days starting on day 1. Cisplatin at a dosage of 6 mg/kg or its vehicle (saline) was administered intraperitoneally as a single injection on day 3, 30 minutes after PARP inhibitor was administered. Combination with carboplatin was conducted in a similar way in MX-1 model in which BMN 673 was administered *per os* once daily for either 8 days or 5 days and carboplatin was injected intraperitoneally at single dose of 35 mg/kg, 30 minutes after BMN 673 on day 3.

PAR assay *in vivo*

MX-1 tumor xenografts were prepared as described in Materials and Methods. When tumors reached an average volume of approximately 150 mm^3, olaparib (100 mg/kg), BMN 673 (1 mg/kg), or vehicle was administered in a single *per os* dosing. Tumors were harvested at 2, 8, and 24 hours after drug dosing, snap-frozen in liquid nitrogen. Tumor tissue was then homogenized in PBS on ice and extracted with lysis buffer (25 mmol/L Tris pH 8.0, 150 mmol/L NaCl, 5 mmol/L EDTA, 2 mmol/L EGTA, 25 mmol/L NaF, 2 mmol/L Na_3VO_4, 1 mmol/L Pefabloc, 1% Triton X-100, and protease inhibitor cocktail) containing 1% SDS. Levels of PAR in the tumor lysates were determined by ELISA using PARP *in vivo* PD Assay II kit (Trevigen).

Disclosure of Potential Conflicts of Interest

L.E. Post, Y. Shen, Y. Feng and B. Wang have ownership interest (including patents) in BioMarin Pharmaceutical Inc. A. Ashworth and C.J. Lord may benefit financially from the development of PARP inhibitors through patents held jointly with AstraZeneca through the Institute of Cancer Research's rewards to inventors scheme. No potential conflicts of interest were disclosed by the other authors.

Authors' Contributions

Conception and design: Y. Shen, F.L. Rehman, C.J. Lord, L.E. Post, A. Ashworth

Development of methodology: Y. Shen, Y. Feng, C.J. Lord

Acquisition of data (provided animals, acquired and managed patients, provided facilities, etc.): F.L. Rehman, J. Boshuizen, R. Elliott, C.J. Lord, A. Ashworth

Analysis and interpretation of data (e.g., statistical analysis, biostatistics, computational analysis): Y. Shen, F.L. Rehman, Y. Feng, C.J. Lord, L.E. Post, A. Ashworth

Writing, review, and/or revision of the manuscript: Y. Shen, F.L. Rehman, Y. Feng, C.J. Lord, L.E. Post, A. Ashworth
Administrative, technical, or material support (i.e., reporting or organizing data, constructing databases): Y. Shen, I. Bajrami
Study supervision: Y. Shen, Y. Feng, C.J. Lord, A. Ashworth
Compound invention: B. Wang

Acknowledgments

The authors thank Drs. Daniel Chu and Peter Myers for their excellent scientific input and continuous support throughout this work; Shanghai HD Biosciences, Inc. for developing and conducting *in vitro* and *in vivo* assays, Shanghai ChemPartner for chemistry work and BiaCore kinetics work; Drs. Mika Aoyagi-Scharber and Paul Fitzpatrick for generating PARP1 protein for the BiaCore study; Dr. Myron Jacobson for excellent scientific discussion and helping with running the PARP2 assay; Dr. Bill Wold (Southern Research Institute, Birmingham, AL) for insightful discussion about animal xenograft models.

Grant Support

Part of this work was funded by Breakthrough Breast Cancer, Cancer Research UK, and the AACR as part of the SU2C Breast Cancer Dream Team initiative. F.L. Rehman is a Breakthrough Breast Cancer Avon Clinical Fellow and is funded as part of the Avon Breast Cancer Crusade. The authors also acknowledge NHS funding to the NIHR Royal Marsden Hospital Biomedical Research Centre.

The costs of publication of this article were defrayed in part by the payment of page charges. This article must therefore be hereby marked *advertisement* in accordance with 18 U.S.C. Section 1734 solely to indicate this fact.

Received May 23, 2013; accepted July 1, 2013; published OnlineFirst July 23, 2013.

References

1. Hoeijmakers JHJ. DNA damage, aging, and cancer. N Engl J Med 2009;361:1475–85.
2. Helleday T, Petermann E, Lundin C, Hodgson B, Sharma RA. DNA repair pathways as targets for cancer therapy. Nat Rev Cancer 2008;8:193–204.
3. Rouleau M, Patel A, Hendzel MJ, Kaufmann SH, Poirier GG. PARP inhibition: PARP1 and beyond. Nat Rev Cancer 2010;10:293–301.
4. Lord CJ, Ashworth A. The DNA damage response and cancer therapy. Nature 2012;481:287–94.
5. Ashworth A. A synthetic lethal therapeutic approach: poly(ADP) ribose polymerase inhibitors for the treatment of cancers deficient in DNA double-strand break repair. J Clin Oncol 2008;26:3785–90.
6. Farmer H, McCabe N, Lord CJ, Tutt ANJ, Johnson DA, Richardson TB, et al. Targeting the DNA repair defect in BRCA mutant cells as a therapeutic strategy. Nature 2005;434:917–21.
7. Bryant HE, Schultz N, Thomas HD, Parker KM, Flower D, Lopez E, et al. Specific killing of BRCA2-deficient tumours with inhibitors of poly (ADP-ribose) polymerase. Nature 2005;434:913–7.
8. Fong PC, Boss DS, Yap TA, Tutt A, Wu P, Mergui-Roelvink M, et al. Inhibition of poly(ADP-ribose) polymerase in tumors from BRCA mutation carriers. N Engl J Med 2009;361:123–34.
9. Audeh MW, Carmichael J, Penson RT, Friedlander M, Powell B, Bell-McGuinn KM, et al. Oral poly(ADP-ribose) polymerase inhibitor olaparib in patients with BRCA1 or BRCA2 mutations and recurrent ovarian cancer: a proof-of-concept trial. Lancet 2010; 376:245–51.
10. Tutt A, Robson M, Garber JE, Domchek SM, Audeh MW, Weitzel JN, et al. Oral poly(ADP-ribose) polymerase inhibitor olaparib in patients with BRCA1 or BRCA2 mutations and advanced breast cancer: a proof-of-concept trial. Lancet 2010;376:235–44.
11. Ledermann J, Harter P, Gourley C, Friedlander M, Vergote I, Rustin G, et al. Olaparib maintenance therapy in platinum-sensitive relapsed ovarian cancer. N Engl J Med 2012;366:1382–92.
12. Calabrese CR, Almassy R, Barton S, Batey MA, Calvert AH, Canan-Koch S, et al. Anticancer chemosensitization and radiosensitization by the novel poly(ADP-ribose) polymerase-1 inhibitor AG14361. J Natl Cancer Inst 2004;96:56–67.
13. Smith LM, Willmore E, Austin CA, Curtin NJ. The novel poly(ADP-Ribose) polymerase inhibitor, AG14361, sensitizes cells to topoisomerase I poisons by increasing the persistence of DNA strand breaks. Clin Cancer Res 2005;11:8449–57.
14. Oliver AW, Amé J-C, Roe SM, Good V, De Murcia G, Pearl LH. Crystal structure of the catalytic fragment of murine poly(ADP-ribose) polymerase-2. Nucleic Acids Res 2004;32:456–64.
15. Schreiber V, Dantzer F, Ame J-C, de Murcia G. Poly(ADP-ribose): novel functions for an old molecule. Nat Rev Mol Cell Biol 2006;7: 517–28.
16. McCabe N, Turner NC, Lord CJ, Kluzek K, Bialkowska A, Swift S, et al. Deficiency in the repair of DNA damage by homologous recombination and sensitivity to poly(ADP-ribose) polymerase inhibition. Cancer Res 2006;66:8109–15.
17. Turner NC, Lord CJ, Iorns E, Brough R, Swift S, Elliott R, et al. A synthetic lethal siRNA screen identifying genes mediating sensitivity to a PARP inhibitor. EMBO J 2008;27:1368–77.
18. Lord CJ, McDonald S, Swift S, Turner NC, Ashworth A. A high-throughput RNA interference screen for DNA repair determinants of PARP inhibitor sensitivity. DNA Repair 2008;7:2010–9.
19. Mendes-Pereira AM, Martin SA, Brough R, McCarthy A, Taylor JR, Kim J-S, et al. Synthetic lethal targeting of PTEN mutant cells with PARP inhibitors. EMBO Mol Med 2009;1:315–22.
20. Foray N, Marot D, Gabriel A, Randrianarison V, Carr AM, Perricaudet M, et al. A subset of ATM- and ATR-dependent phosphorylation events requires the BRCA1 protein. EMBO J 2003;22: 2860–71.
21. Hucl T, Rago C, Gallmeier E, Brody JR, Gorospe M, Kern SE. A syngeneic variance library for functional annotation of human variation: application to BRCA2. Cancer Res 2008;68:5023–30.
22. Murai J, Huang S-YN, Das BB, Renaud A, Zhang Y, Doroshow JH, et al. Trapping of PARP1 and PARP2 by clinical PARP inhibitors. Cancer Res 2012;72:5588–99.
23. Redon CE, Nakamura AJ, Zhang Y-W, Ji JJ, Bonner WM, Kinders RJ, et al. Histone gammaH2AX and poly(ADP-ribose) as clinical pharmacodynamic biomarkers. Clin Cancer Res 2010;16:4532–42.
24. Donawho CK, Luo Y, Luo Y, Penning TD, Bauch JL, Bouska JJ, et al. ABT-888, an orally active poly(ADP-ribose) polymerase inhibitor that potentiates DNA-damaging agents in preclinical tumor models. Clin Cancer Res 2007;13:2728–37.
25. Kummar S, Chen A, Parchment RE, Kinders RJ, Ji J, Tomaszewski JE, et al. Advances in using PARP inhibitors to treat cancer. BMC Med 2012;10:25.
26. Boulton S, Pemberton LC, Porteous JK, Curtin NJ, Griffin RJ, Golding BT, et al. Potentiation of temozolomide-induced cytotoxicity: a comparative study of the biological effects of poly(ADP-ribose) polymerase inhibitors. Br J Cancer 1995;72:849–56.
27. Delaney CA, Wang LZ, Kyle S, White AW, Calvert AH, Curtin NJ, et al. Potentiation of temozolomide and topotecan growth inhibition and cytotoxicity by novel poly(adenosine diphosphoribose) polymerase inhibitors in a panel of human tumor cell lines. Clin Cancer Res 2000;6:2860–7.
28. Plummer R, Jones C, Middleton M, Wilson R, Evans J, Olsen A, et al. Phase I study of the poly(ADP-Ribose) polymerase inhibitor, AG014699, in combination with temozolomide in patients with advanced solid tumors. Clin Cancer Res 2008;14:7917–23.
29. Palma JP, Wang Y-C, Rodriguez LE, Montgomery D, Ellis PA, Bukofzer G, et al. ABT-888 confers broad *in vivo* activity in combination with temozolomide in diverse tumors. Clin Cancer Res 2009;15:7277–90.
30. Balmaña J, Tung NM, Isakoff SJ, Graña B, Ryan PD, Rafi R, et al. Phase I, open-label study of olaparib plus cisplatin in patients with advanced solid tumors. J Clin Oncol 30, 2012 (suppl; abstr 1009).
31. Dent RA, Lindeman GJ, Clemons M, Wildiers H, Chan A, McCarthy NJ, et al. Safety and efficacy of the oral PARP inhibitor olaparib (AZD2281)

in combination with paclitaxel for the first- or second-line treatment of patients with metastatic triple-negative breast cancer: results from the safety cohort of a phase I/II multicenter trial. J Clin Oncol 28:15s, 2010 (suppl; abstr 1018).

32. Balmana J, Domchek SM, Tutt A, Garber JE. Stumbling blocks on the path to personalized medicine in breast cancer: the case of PARP inhibitors for BRCA1/2-associated cancers. Cancer Discov 2011;1:29–34.
33. Chu D, Wang Binventors; BioMarin Pharmaceutical Inc., assignee. Dihydropyridophthalazinone inhibitors of poly(ADP-ribose) polymersase (PARP). United States patent US 8012976. 2011 Sep 6.
34. Wang B, Chu D, Liu Y, Jiang Q, Lu Linventors; BioMarin Pharmaceutical Inc., assignee. Processes of synthesizing dihydropyridophthalazinone derivatives. PTC WO 2011/097602. 2011 Aug 1.
35. Menear KA, Adcock C, Boulter R, Cockcroft XL, Copsey L, Cranston A, et al. 4-[3-(4-cyclopropanecarbonylpiperazine-1-carbonyl)-4-fluorobenzyl]-2H-phthalazin-1-one: a novel bioavailable inhibitor of poly(ADP-ribose) polymerase-1. J Med Chem 2008;51:6581–91.
36. Canan Koch SS, Thoresen LH, Tikhe JG, Maegley KA, Almassy RJ, Li J, et al. Novel tricyclic poly(ADP-ribose) polymerase-1 inhibitors with potent anticancer chemopotentiating activity: design, synthesis, and X-ray cocrystal structure. J Med Chem 2002;45:4961–74.
37. Zhu G-D, Gong J, Gandhi VB, Penning TD, Giranda VLinventors; Gandhi VB, Giranda VL, Gong J, Penning TD, Zhu G-D, assignees. 1H-benzimidazole-4-carboxamides substituted with a quaternary carbon at the 2-position are potent PARP inhibitors. United States patent application 2006/0229289. 2006 Oct 2006.